





Phosphorus chemistry in plant charcoal: interplay between biomass composition and thermal condition

Yudi Wu^A, Lois M. Pae^A and Rixiang Huang^{A,*}

For full list of author affiliations and declarations see end of paper

*Correspondence to:

Rixiang Huang
Department of Environmental and
Sustainable Engineering, University at
Albany, 1400 Washington Avenue, Albany,
NY 12222, USA

Email: rhuang6@albany.edu

Received: 20 June 2023 Accepted: 29 November 2023 Published: 18 December 2023

Cite this:

Wu Y et al. (2024) International Journal of Wildland Fire 33, WF23096. doi:10.1071/WF23096

© 2024 The Author(s) (or their employer(s)). Published by CSIRO Publishing on behalf of IAWF. This is an open access article distributed under the Creative Commons Attribution-NonCommercial-NoDerivatives 4.0 International License (CC BY-NC-ND)

OPEN ACCESS

ABSTRACT

Background. Vegetation fire may change Phosphorus (P) cycling in terrestrial ecosystems through converting biomass into fire residues. Aim. The aim of this study was to understand the chemistry and mobility of P in fire residues to help reveal P thermochemistry during biomass burning and post-fire P cycling. Methods. A combination of sequential extraction, liquid 31P NMR and P K-edge XANES was used to obtain quantitative P speciation and explain P solubilisation behaviours of charcoal. Key results. Despite varying diverse P species existing in raw biomass, only two P structural moieties - orthophosphate and pyrophosphate - were identified in charcoal. However, relative abundance of pyrophosphate differs greatly among charcoal samples from different biomass types, ranging between 0 and 40% of total extractable P. Although P K-edge XANES data indicates abundant soluble phosphate minerals, most P (70–90%) is likely occluded physically in the charcoal. The bicarbonate-extractable P (the Olsen-P) varies significantly and cannot be explained by surface P concentration or elemental stoichiometry alone. Conclusion and implications. The results suggest the importance of starting biomass P speciation (i.e. molecular structure and complexation environment) and thermal conditions in controlling P speciation and availability in charcoal. The different P chemistry between charcoal and ash suggests the importance of fire types and severity in disturbing the P cycle.

Keywords: ash, charcoal, elemental speciation, fire, mobility, phosphorus cycling, temperate ecosystem, XANES.

Introduction

Phosphorus (P) is commonly limited in most natural terrestrial ecosystems (Du et al. 2020; Hou et al. 2020). Soil P availability relies heavily on recycling P from biomass, and the recycling is highly efficient in mature ecosystems (Sohrt et al. 2017). This is evidenced by the relatively small P export via surface runoff and leaching (which is comparable to the flux of system input via atmospheric deposition and weathering) and the large contributions of P from organic matter mineralisation to total plant uptake (e.g. 80% in a boreal forest) (Yu et al. 2018). By burning living and dead biomass and changing the physical, chemical and biological characteristics of the burned ecosystems, vegetation fire is expected to change the cycling of many elements, particularly macronutrients like P, for which internal recycling of the biomass pool is relatively important (Hart et al. 2005). The burning of biomass and production of solid residues (i.e. charcoal and ash, being the incomplete and complete combustion products, respectively) represent the main direct and immediate change to P cycling, because it changes the physical and chemical forms of the aboveground P pools that affect the post-fire P cycling. Phosphorus exists abundantly as various organic species in biomass (such as inositol phosphate, phosphate monoesters and phosphate diesters), and their mineralisation and release from the organic matrix are mediated primarily by microbes (Turner et al. 2007; Pistocchi et al. 2018). With the transformation of biomass into ash and charcoal, organic P (P_o) is extensively mineralised and P is embedded in matrices different from biomass (Gray and Dighton 2006). As a result, cycling pathways (e.g. transport in soil and surface runoff) and fluxes of this aboveground P pool can change, affecting soil P status and P export from the burned environment to water bodies. For example, soil P contents and pools were found to change after fire (Butler *et al.* 2018), and fire is known to enhance P export from the burned environment to water bodies (Bayley *et al.* 1992; McEachern *et al.* 2000), in which the cycling of P in fire residues may play a significant role.

Considering the significance of post-fire cycling of P in fire residues, it is important to understand their P chemistry, particularly considering the vast diversity of biomass fuel types and variable fire conditions that primarily control the properties of fire residues. Many studies have characterised P chemistry in fire residues that are either directly collected from the field or prepared in the lab, while a mechanistic understanding remains lacking. First, although extensive studies have characterised the chemical forms of P, highly variable results were found and the impacts of biomass types and fire conditions are not quantitatively understood. For example, variable P molecular structures (e.g. pyrophosphates and organophosphates) were identified in fire residues (García-Oliva et al. 2018; Santín et al. 2018), but thermochemical reactions and factors controlling their formation and abundance remain unknown. Second, although P mobility of fire residues has been evaluated, mechanisms underlining the rate and extent of P release are not well understood (Qian et al. 2009; Galang et al. 2010). For example, percentages of soluble orthophosphate (Pi) vary greatly among residues derived from different plant species, while the cause was unclear (Schaller et al. 2015). Such knowledge gaps impede our ability to gain a systematic understanding of the thermochemistry of P during vegetation fire and to predict the impact of fire on P cycling.

This study aims to fill the knowledge gaps by examining P speciation and P availability in charcoal across a wide range of plant species and parts, as well as thermal conditions. Herein, fire residue refers to all forms of burning products, and charcoal and ash refer specifically to the incomplete and complete burning products, respectively. We specifically focus on charcoal because: (1) charcoal is part of the fire residues deposited on soils and is a reservoir of nutrients (Marañón-Jiménez et al. 2013); and (2) charcoal is a carbonaceous material, whose composition and property are different from that of the complete burning product - ash (which consists of only inorganics). As shown in our separate study on ash, P was completely mineralised and existed as various phosphates, whose solubility primarily controls P solubility (Wu et al. 2023). We hypothesise that biomass P speciation and elemental stoichiometry largely determine P speciation in charcoal, and P availability is controlled by both P chemical speciation and charcoal surface property. To obtain detailed P speciation and explore P transformation during pyrolysis, complementary P analyses – liquid ³¹P nuclear magnetic resonance spectroscopy (NMR), P K-edge absorption near edge structure (XANES) and a modified

Hedley sequential extraction – are used. Availability of P (estimated by bicarbonate extraction) is further correlated with different physicochemical properties of charcoal, including chemical composition and surface characteristics. Although some studies had characterised detailed P speciation in a thermosequence of chars using both NMR and sequential extraction, the focus was on a few crop biomass and organic wastes that are different from biomass burned in natural ecosystems (Uchimiya and Hiradate 2014; Xu et al. 2016; Sun et al. 2018). This study is the first to examine a large set of tree species and compartments, relating biomass composition, thermal conditions and charcoal property, which can help reveal the reactions and factors controlling charcoal P chemistry.

Materials and methods

Sampling

Plant fruit (i.e. cone), wood (i.e. twig and bark) and leaf (i.e. needle) parts of *Pinus rigida* (pitch pine) and *Pinus strobus* (white pine) were collected from the Albany Pine Bush Preserve, and *Picea abies* (Norway spruce) cone and needle were collected from the Five Rivers Environmental Education Center, both located in Albany, New York. Leaf, wood and bark of deciduous trees, including *Quercus rubra* (red oak), *Quercus alba* (white oak), *Acer rubrum* (red maple) and *Fagus* (beech), were collected from a residential neighbourhood, also in Albany. Specifically, wood parts (bark, twig and hardwood) were collected from living plants during tree cutting. The biomass was dried in an oven at 70°C until there was no further weight change, then pulverised using a blender. Detailed summary of all biomass types used in this work is included in Table 1.

Preparation of charcoal and natural fire residue samples

The pulverised biomass was compacted in glass containers, wrapped with aluminium foil and buried in a sand bucket (at least 10 cm below the surface), which was heated in a benchtop muffle furnace (Thermolyne, Thermos Scientific). Because the focus of this work is to compare charcoal P chemistry across a wide range of plant species and parts, charcoal samples (n = 22) were produced consistently under controlled thermal conditions (pyrolysis temperatures 300, 450, and 600 °C for 6-8 h). The samples were labelled as: biomass abbreviation + pyrolysis temperature. For example, SC600 was for charcoal from pyrolysis of spruce cone at 600°C. Details of sample labelling can be found in Table 1. In addition, in order to demonstrate the relationship between combustion completeness and P mobility, three sets of burning residues were also included: (1) complete burning products – ash samples (n = 2) that were produced from spruce cone and red oak wood in air at 550 °C for ~6 h

Table I. Production temperature, labelling and chemical characteristics of charcoal samples analysed in this work.

Plants	Plant parts	Temperature (°C)	Sample label	Char yield (%)	Surface area (m²/g)	P (mg/ kg)	Ca/P molar ratio	Mg/P molar ratio	K/P molar ratio	Na/P molar ratio
Pitch pine	Cone	300	PPC300	49.8 ± 0.4	-	373.9	4.8	1.5	0.8	0.2
	Cone	450	PPC450	36.0 ± 0.5	-	516.8	4.8	1.5	0.8	0.2
	Cone	600	PPC600	29.9 ± 0.5	-	622.4	4.8	1.5	8.0	0.2
	Needle	600	PPN600	29.6 ± 1.1	-	1327.9	9.4	2.0	1.2	0.2
	Twig	600	PPT600	32.8 ± 0.2	451	814.7	6.0	1.2	0.6	0.3
	Bark	600	PPB600	40.0 ± 0.2	524	337.5	9.0	0.8	1.2	0.4
White pine	Cone	600	WPC600	29.6 ± 1.3	-	1000.8	5.6	3.0	4.7	0.3
	Needle	600	WPN600	30.4 ± 0.2	426	1117.5	10.9	2.8	1.1	0.1
Spruce	Cone	300	SC300	51.6 ± 0.1	-	996.2	1.8	1.6	5.6	0.2
	Cone	450	SC450	36.1 ± 0.1	-	1423.9	1.8	1.6	5.6	0.2
	Cone	600	SC600	30.7 ± 0.1	131	1676.3	1.8	1.6	5.6	0.2
	Needle	600	SN600	31.6 ± 0.4	85	3166.7	7.3	0.9	3.7	1.0
Beech	Leaf	600	BF600	32.5 ± 0.4	-	1149.6	20.9	1.6	1.3	5.3
White oak	Leaf	600	WOL600	33.0 ± 0.4	-	1105.4	28.3	2.7	1.5	1.1
Red oak	Leaf	600	ROL600	30.5 ± 0.1	283	2246.5	12.7	2.8	1.5	0.8
	Wood	600	ROW600	24.4 ± 0.1	_	943.0	29.4	1.7	5.0	0.1
	Bark	300	ROB300	58.0 ± 0.6	_	311.6	159.2	2.3	5.3	0.1
	Bark	450	ROB450	35.5 ± 0.3	_	509.2	159.2	2.3	5.3	0.1
	Bark	600	ROB600	32.4 ± 0.1	-	557.7	159.2	2.3	5.3	0.1
Red maple	Leaf	600	RML600	33.0 ± 0.2	-	1543.4	22.2	3.1	1.6	0.3
	Wood	600	RMW600	26.7 ± 0.6	-	612.1	8.9	1.9	5.3	0.1
	Bark	600	RMB600	34.8 ± 0.4	-	890.1	33.9	1.8	4.2	0.1

(Wu *et al.* 2023); (2) mixed fire residue samples (n = 2) that were produced from igniting spruce cone and red oak wood in air, simulating natural fire conditions; and (3) burning residues (n = 5) from generators that burn woods (provided by Resource Management, Inc.). These samples represent realistic fire burning products from varying burning conditions and consist of both charcoal and ash. Combustion completeness of these samples was evaluated based on mass recovery and total Carbon (C) content of residues.

Characterisation of physicochemical properties of charcoal

Biomass elemental composition (C, H, N, S) was determined by an CHNS Elemental Analyser (2400 Series II, PerkinElmer Inc, USA). Analysis of total P and other macronutrients (i.e. K, Ca, Na, Mg, Mn, Al, and Fe) in biomass samples was performed by the Cornell Nutrient Analysis Laboratory. The elements were solubilised using a hotplate digestion method and determined by inductively coupled plasma—optical emission spectrometry (ICP-OES) following the EPA Method No. 6010-B. Elemental contents (P and metals) in charcoal were calculated based on the mass recovery (i.e. char yield) of each biomass type, because these macronutrients are assumed to completely remain in charcoal due to their high volatilisation temperatures (>750 °C) (Bodí et al. 2014). Thus, total P in charcoal was calculated using the following equation: Total P in charcoal (mg kg $^{-1}$) = Total P in Biomass/char yield. Contents of K, Ca, Na and Mg in charcoal were also calculated similarly. Brunauer, Emmett and Teller (BET) specific surface area (SSA, N₂ adsorption) of selected charcoal samples (Table 1) from different biomass samples yet the same production temperature (e.g., 600°C) was measured using a gas adsorption analyser (3Flex, Micromeritics, Inc.).

Solution extraction of P

Measurement of mobile P and its release kinetics

Olsen-P content was determined for selected charcoal samples (n = 19) and burning residue samples (n = 7) (Olsen 1954). A designated amount of the samples (1.5 g) was mixed with 100 mL 0.5 M NaHCO₃ solution in a 125 mL

glass bottle. The bottle was capped and continuously agitated at 120 rpm and room temperature (20 °C). Kinetics of the Olsen-P release was determined for 7 of the 19 charcoal samples, and 3 mL of samples was withdrawn at specific time intervals (0.5, 1, 2, 3, 4, 8, 12, 24, 48 and 120 h) and filtered through a 0.45 μ m (nylon) membrane. Phosphate content in the solution was analysed using the ascorbic acid assay on a UV-vis spectrophotometer (UV-1900, Shimadzu). For each time point, the released P fraction (Polsen, %) was calculated using the following equation:

$$P_{\text{olsen}} = \frac{C_x V}{C_P m}$$

where C_X (mg L⁻¹) is the P concentration in solution, V is the volume of NaHCO₃ solution (L), C_p is the total P concentration in charcoal (mg kg⁻¹) and m is the mass of added charcoal (g). The temporal release data was fitted by the pseudo-first-order, pseudo-second order and simple Elovich equations, to interpret the P release pattern. Goodness of fit was evaluated by coefficients of determination (R^2) and standard deviation. Data for ash of spruce cone and red oak wood from our previous study were also included for comparison (Wu *et al.* 2023).

Modified Hedley sequential extraction

Sequential fractionation of P in charcoals (n=19) was conducted in replicate, following the modified Hedley sequential extraction method (Gu *et al.* 2020). Specifically, 1.5 g of charcoal was added to a 50 mL polypropylene centrifuge tube and sequentially extracted by 30 mL extraction solutions: deionised water, followed by 0.5 M NaHCO₃, 0.1 M NaOH and 1 M HCl. The sample tubes were continuously shaken at 120 rpm at room temperature, and at the end of each step, the tubes were centrifuged at 3750 rpm for 20 min to separate the liquid and solid. Inorganic P content (Pi) and total P contents (after persulfate digestion (Gu *et al.* 2020)) in the extracted liquid were determined using the ascorbic acid assay (Hedley *et al.* 1982). Organic P content was calculated as the difference between total P and Pi. Relative abundance of P in each extraction pool was expressed as % of total P in the charcoal.

Characterisation of P speciation

Molecular moieties and complexation states of P in biomass and charcoal samples were characterised using 31 P liquid NMR (n=6 for biomass samples, n=14 for charcoal samples) and P K-edge XANES (n=1 for biomass samples, n=12 for charcoal samples).

Liquid ³¹P NMR analysis

Charcoal and biomass samples were extracted using a solution containing 0.25 M NaOH and 0.05 M EDTA, and P species in the solution was characterised by ^{31}P NMR. The solid to liquid ratios used were 1.5:15 and 5:15 g mL $^{-1}$, for charcoal and biomass, respectively. The liquid was

separated and lyophilised, then re-dissolved in 700 μ L 1 M NaOH with 10% deuterium oxide (D₂O) for ³¹P NMR analysis (Turner *et al.* 2003; Cade-Menun 2005). NMR spectra of each sample was collected using a Bruker AMX 500 MHz spectrometer operated at 203 MHz at 297 K. The parameters used were: 90° pulse width, 6.5k data points (TD) over an acquisition time of 0.40 s and relaxation delay of 2 s. 4096 scans were acquired for each biomass sample and 1024 scans were required for each charcoal sample.

Phosphorus K-edge X-ray absorption near-edge structure spectroscopy (XANES)

Phosphorus K-edge XANES data of biomass and charcoal samples were collected at the Tender Energy X-ray Absorption Spectroscopy (TES) beamline at the National Synchrotron Light Source II at Brookhaven National Lab (Upton, NY). Selected charcoal and biomass samples (Spruce cone biomass and its charcoal samples and other charcoal samples produced at 600°C; Table S1) were pulverised before spreading on a P-free carbon tape (mounted onto a sample holder) for XANES spectra collection. The data were collected in the fluorescence mode using a four-element Si(Li) drift detector. Two scans were collected for each sample. The spectra were collected from 2120 to 2240 eV, with the following steps: 2 eV for 2120-2140 eV; 0.3 eV for 2140.5-2190 eV; and 1 eV for 2190-2240 eV. The duplicated spectra were merged, background subtracted and normalised, before linear combination fitting (LCF). All analyses were performed using the Athena package.

Phosphorus speciation was estimated by LCF of the processed XANES spectra at an energy range from 2140 to 2200 eV. The reference compounds were selected based on elemental composition and target transformation analysis. Because Ca, K and Mg are the most abundant cations with a metal to P molar ratio >1, their phosphate minerals are the most likely species in charcoal. Phytic acid was selected to represent organophosphates. Target transformation analysis was performed to further shortlist the references, and spectra of the following compounds were selected: (1) amorphous calcium phosphate (ACP); (2) hydroxyapatite (HAP); (3) monopotassium phosphate; (4) trimagnesium phosphate octahydrate (Mg₃(PO₄)₂); (5) dimagnesium phosphate trihydrate (MgHPO₄); (6) ammonium magnesium phosphate hexahydrate (struvite); and (7) phytic acid. Details of these reference compounds can be found in our previous study. The goodness of fit was evaluated using the residual factor (R factor), and the fit with smallest R factor was deemed best fit.

Results and discussions

Physical and chemical properties of biomass and charcoal

Parts of representative coniferous and deciduous trees were selected to produce charcoal at temperature from 300 to 600 °C, resulting in charcoals with a range of physicochemical

properties (Table 1 and Supplementary Table S2). This enabled the testing of our hypothesis that biomass composition (specifically starting P species and elemental stoichiometry) and pyrolysis temperature control P speciation and mobility of charcoals. For example, P content in the selected biomass ranges from 135 to 1000 mg kg⁻¹, and that of other macro-nutrients (e.g. Ca, K, Mg and Na) also varies for more than an order of magnitude. The varying elemental contents resulted in a big range of metal-to-P molar ratios, with Ca/P ranging from 1.8 to 160, K/P from 0.6 to 5.6 and Mg/P from 0.8 to 3.1 (Table 1).

P speciation in biomass and charcoal

Detailed P speciation, including molecular structure and complexation environment, was characterised for biomass and charcoal, to explore the thermochemical mechanisms of P

transformation during incomplete combustion and the impacts of fuel composition and thermal condition. Overall, all biomass types consist of diverse molecular structures, whose relative abundance varies among different plant species (for the same compartment) and different compartments (for the same species) (Fig. 1). The P molecules identified (by ³¹P liquid NMR) include orthophosphate, phosphatemonoester and -diester, pyrophosphate and polyphosphates (Fig. 1), which are typical P species presented in plants (Noack et al. 2014). In the analysed samples, organophosphates (mono- and di-esters) account for about 40-50% of total P. The main difference is the relative abundance of orthophosphate and condensed phosphates: (1) polyphosphate is relatively abundant in the cones and needles of pine trees; and (2) spruce cone and oak wood contain pyrophosphate that is negligible in other biomass samples. Relative abundance of organophosphates and condensed

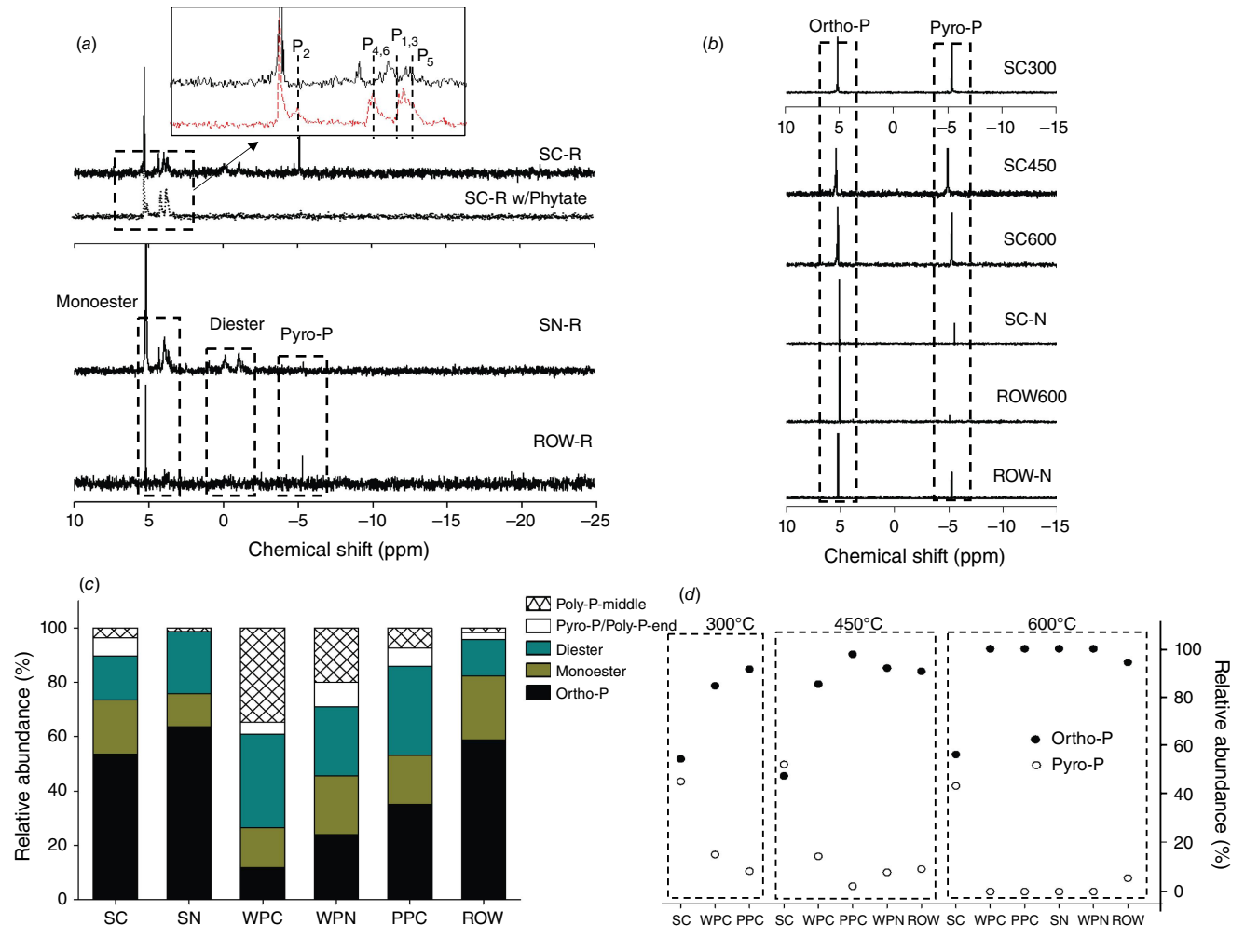


Fig. 1. (a) ³¹P liquid NMR spectra of the extracts from Norway spruce cone (SC-R) and needle (SN-R), red oak wood (ROW-R), spruce cone sample spiked with phytic acid (SC-R w/Phytate). (b) ³¹P NMR spectra of the extracts from charcoal samples of Norway spruce cone and red oak wood produced at 300–600 °C and residue samples from simulated fire condition (SC-N and ROW-N). (c) Relative abundance of different P species in the extracts of raw biomass based on ³¹P NMR peak density. (d) Relative abundance of different P species in charcoal extracts. Description of the charcoal samples can be found in Table 1.

phosphates depends on many factors, such as: (1) physiological functionality of specific P species in the plant parts, e.g. phospholipids, adenosine triphosphate and nucleic acids in cell structure, metabolism and reproduction, respectively; (2) plant growth stage, e.g. leaf senescence (Smith *et al.* 2015); and (3) nutrient status (Hidaka and Kitayama 2011).

Following pyrolysis, only orthophosphate and pyrophosphate were identified, and abundance of pyrophosphate varies among charcoal samples (Fig. 1b, d). For example, abundant pyrophosphate (~40–50%) was found in the extracts of chars derived from Norway spruce cone, regardless of pyrolysis temperature (300–600°C). However, pyrophosphate abundance is relatively small (even absent) in all other tested chars. Similarly, only orthophosphate and pyrophosphate were identified in residues from simulated

burning (SC-N and ROW-N), with pyrophsophate in SC-N more abundant than that in ROW-N. Because ³¹P liquid NMR only identifies and quantifies P structures in liquid extracts, which is a destructive analysis and does not reveal complexation environments of the P structures, P K-edge XANES analysis was used to estimate *in situ* the P species in chars. It is worth noting that LCF of P K-edge XANES data is relatively insensitive (particularly to organophosphates), with fitting errors at ~5–10% for even spectrally distinct mineral species (Werner and Prietzel 2015). Therefore, the XANES data was interpreted semi-quantitatively only. First, XANES data shows a gradual reduction in organophosphate abundance (fitted as phytate) and formation of abundant crystalline calcium phosphates (fitted as hydroxyapatite) in chars (Fig. 2 and Supplementary Table S2). For example, an

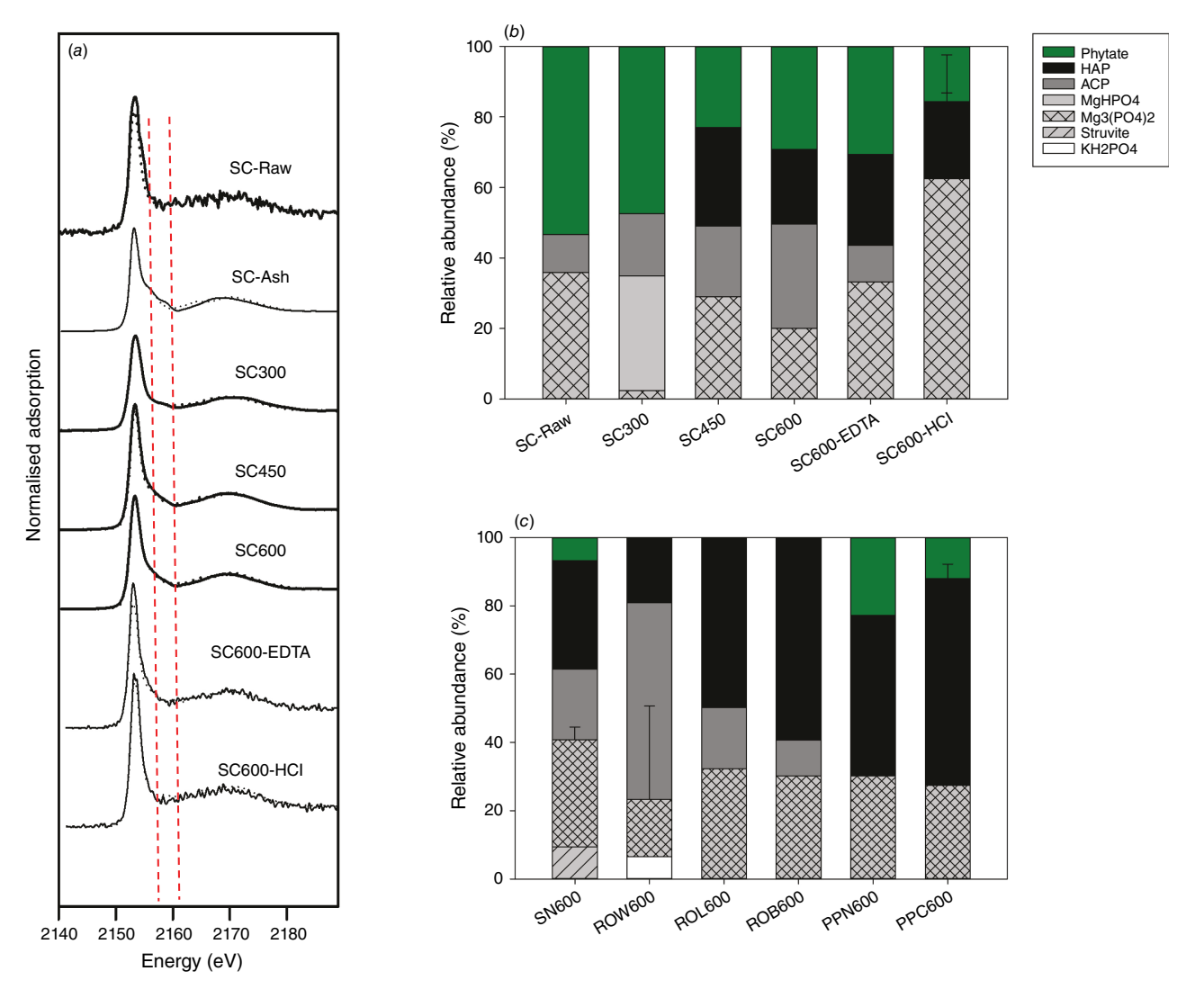


Fig. 2. (a) A series of P K-edge XANES spectra for samples from spruce cone. (b) Relative abundance of P species estimated by LCF of the XANES data of spruce cone samples (raw biomass, chars and 600 °C chars after EDTA or HCl extraction). (c) Relative abundance of P species of charcoal samples produced at 600 °C, including spruce needle (SN), red oak wood (ROW), red oak leaf (ROL), red oak bark (ROB), pitch pine bark (PPB) and pitch pine cone (PPC). Samples with '-EDTA' and '-HCl' represent samples after EDTA and HCl extraction, respectively. Description of the charcoal samples can be found in Table 1.

increasing amount of hydroxyapatite (from 0 to 20%) and a decreasing amount of phytate (from 50 to 30%) were found in spruce cone chars (from 300 to 600 °C). The result is consistent with the ³¹P liquid NMR result showing that organophosphates are mineralised during pyrolysis. Second, although abundant Ca and Mg phosphates were similarly identified in all char samples that agree with the stoichiometric abundance of these elements, their abundance differs among chars. For example, spruce cone chars have relatively low contents of Ca phosphates ($\sim 10-50\%$) compared with other types of charcoals (e.g. from red oak and pitch pine biomass), corresponding to its small Ca/P molar ratio (1.8) (Table 1). Variations in pyrophosphate abundance and crystalline Ca phosphates in chars can be related to initial P speciation in their biomass, which will be discussed in the last Section: Mechanisms of P transformation during burning and impacts on P mobility.

Solubility and dissolution kinetics of charcoal P

P solubility estimated by sequential extraction

Phosphorus speciation and solubility in the chars were also estimated by the modified Hedley extraction, with P of different chemical environments being sequentially extracted by water, NaHCO₃, NaOH and HCl. The residual P possibly represents P in the C matrix that is not accessible or extractable by chemical solutions. Following pyrolysis, P in charcoal was greatly immobilised, as 70–90% are residual P and the labile P (H₂O and NaHCO₃ extractable P) accounts for only 2–15% (Fig. 3). In general, P becomes less available as temperature increases, except for chars of spruce cone, where the labile P increases with temperature (8–15%). Phosphorus extracted in the labile pool is mostly orthophosphate, with

<1% non-orthophosphates (the difference between total P and orthophosphate) in most charcoal. The Po is likely pyrophosphate that was identified in ³¹P NMR, becasue it does not react with molybdate reagent before persulfate digestion (Doolette and Smernik 2011). Only a small P fraction (1–5%) partitions in the NaOH pool, which is consistent with the relatively low Fe and Al abundance (compared with P) and low Fe and Al bound P in the chars. The HCl P pool is relatively abundant (up to 20%), but its pool size varies broadly among chars. As shown in chars of spruce cone, pitch pine cone and red oak bark, the HCl P pool decreases as pyrolysis temperature increases. This is contradictory to the fact that P is increasingly mineralised at increased temperatures, forming more crystalline Ca phosphates as shown by XANES data (Huang et al. 2017). The HCl P pool also varies among 600 °C chars of different biomass types, ranging between 2 and 17%. The large residual P pool and great variations in P partitioning among the sequential extraction pools in chars suggest that compared with chemical speciation, matrix effect is likely to play a more important role in controlling P solubility.

Release kinetics of Olsen-P from charcoal

To further explore the mechanism of P mobilisation from chars, rate and extent of P release during NaHCO $_3$ extraction were measured and correlated with physicochemical properties (i.e. specific surface area and elemental stoichiometry) of the chars (Fig. 4). This NaHCO $_3$ extractable P is exchangeable P (P $_{\rm ex}$) that is considered to be directly bioavailable in soils, also referred to as mobile P or labile P herein (Olsen 1954). As shown in the release rate data, the Olsen-P was rapidly released within the first few hours and stabilised afterwards (Fig. 4a). This suggests similar

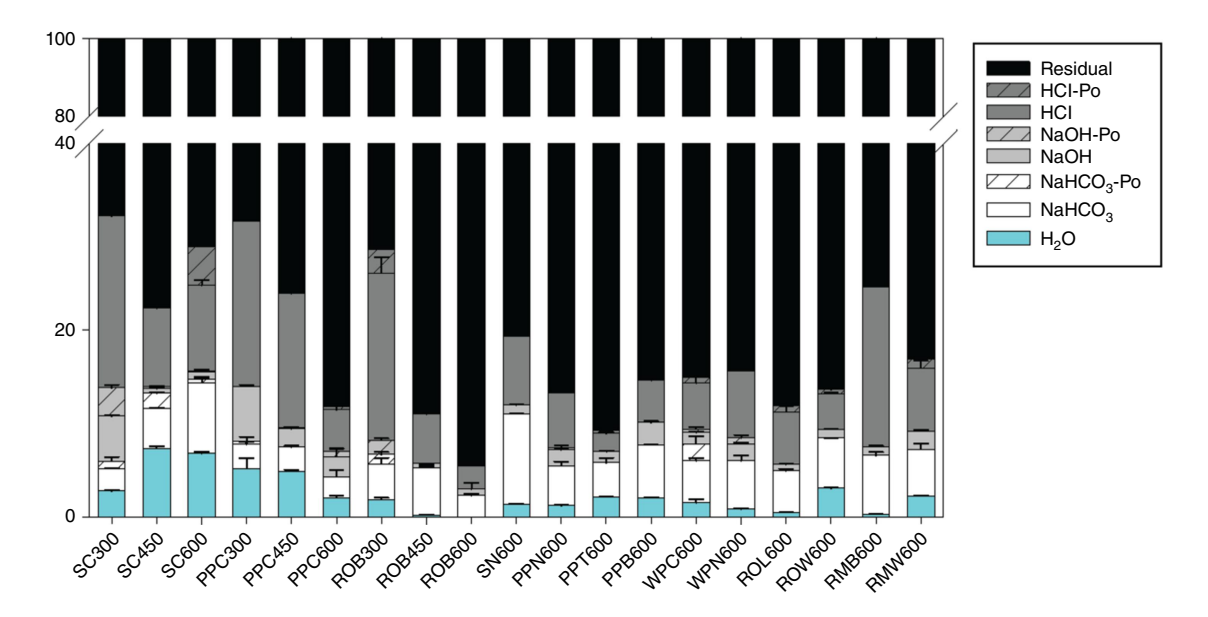


Fig. 3. Partitioning of P in different extraction pools determined by the modified Hedley fractionation method for charcoal samples. Description of the charcoal samples can be found in Table 1.

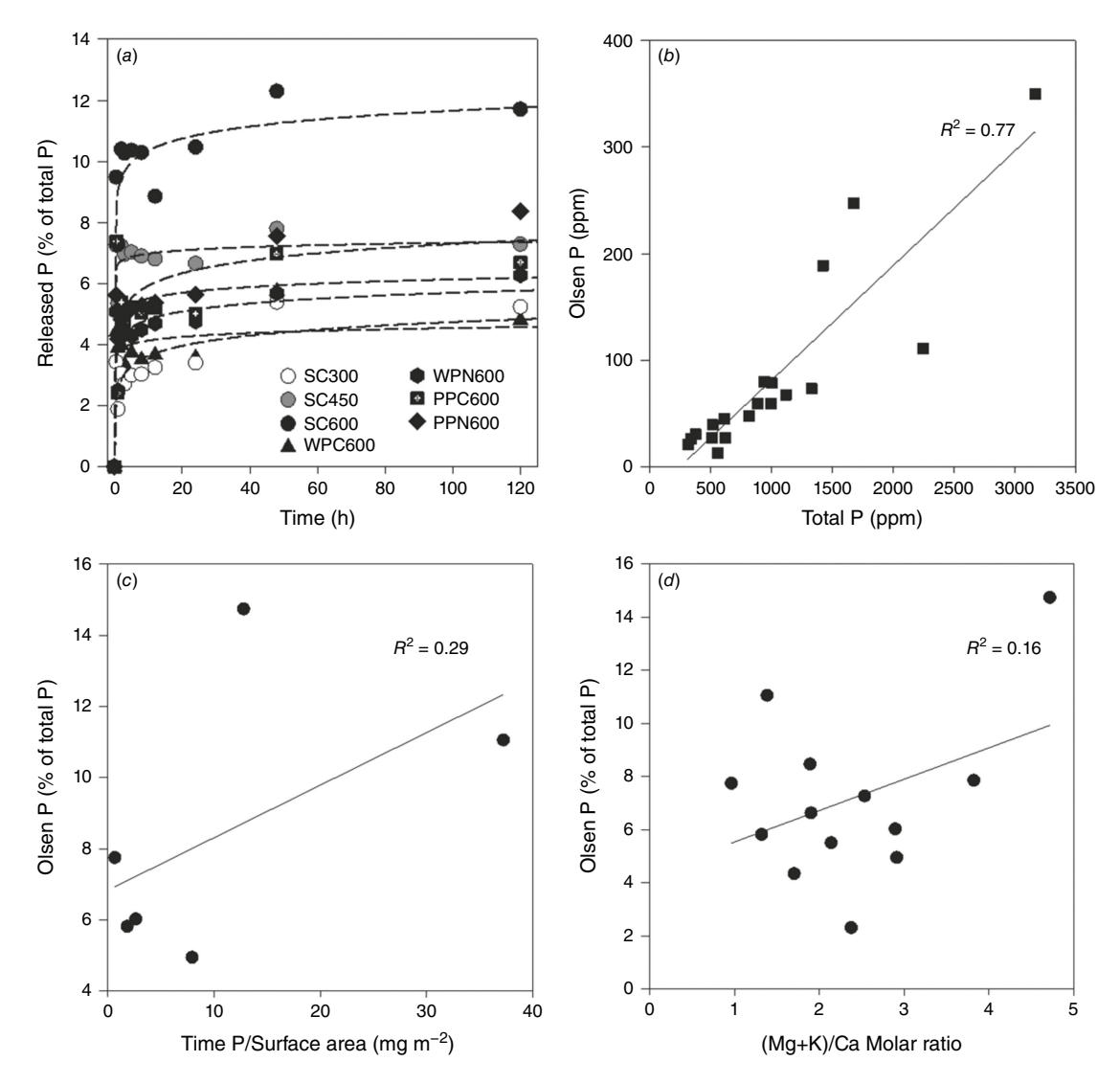


Fig. 4. (a) Temporal release of exchangeable P for selected plant charcoal and its fitting by the simple Elovich equation. (b) Correlation between Olsen-P and total P content. (c) Correlation between Olsen-P and surface P concentration (total P/surface area). (d) Correlation between Olsen-P and (Mg + K)/Ca molar ratio of charcoal samples. Description of the charcoal samples can be found in Table 1.

chemical nature of the $P_{\rm ex}$ among different chars. Three kinetic models (i.e. first order, second order, and simple Elovich equations) were applied to understand the possible release mechanisms. The simple Elovich equation is a best fit because it yields better s.e. and R^2 values (Supplementary Table S3). The simple Elovich equation has been extensively used to describe the desorption/release system, especially when first order equation is insufficient to describe the heterogeneous and multiple desorption/release processes (Chien and Clayton 1980). This Olsen-P pool (approximate to sum of the H_2O and $NaHCO_3$ pools) varies among chars and was found to correlate linearly with the total P (Fig. 4b). However, the percentage of Olsen-P does not correlate with either surface P concentration or the Ca/P molar ratios

(or (Mg + K)/Ca), which represent physical and chemical factors, respectively (Fig. 4c, d).

Impacts of combustion completeness on P chemistry and mobility

Fire varies in intensity and duration, resulting in the formation of fire residues with different properties. One of these is burning completeness, which affects the relative portions of ash and charcoal (Úbeda *et al.* 2009; Pereira *et al.* 2012). A high degree of combustion completeness is characterised by heavy white ash deposition and substantial loss of organic matter, always correlating with a high degree of fire intensity or severity. To evaluate the effect of burning

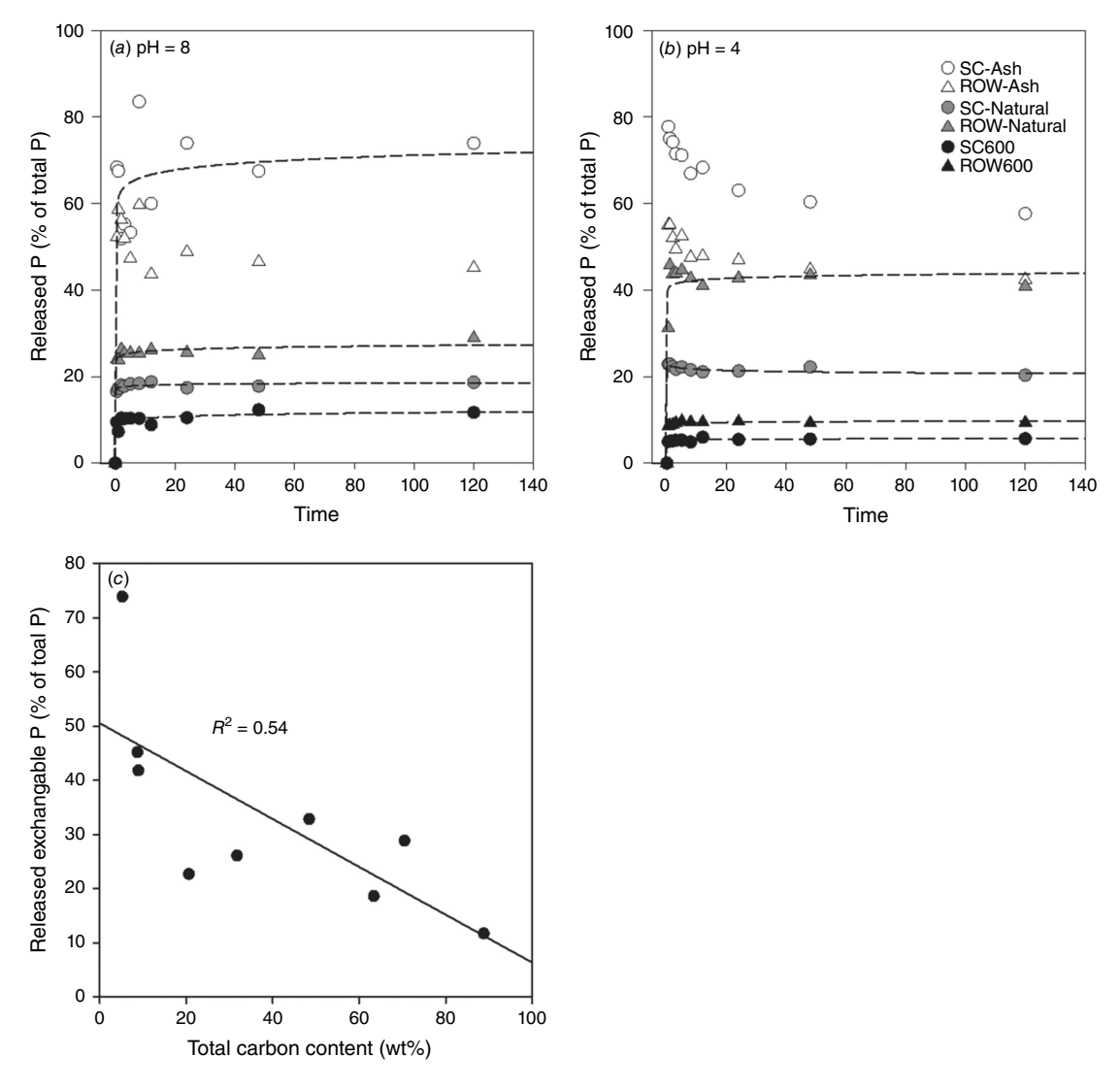


Fig. 5. Phosphate release kinetics for fire residues of different burning completeness at (a) pH 8.0 (0.5 M bicarbonate buffer) and (b) pH 4.0 (0.2 M acetate buffer). (c) Correlation between Olsen-P and total C content (wt%) of fire residues. SC-Natural and ROW-natural refer to residue samples from simulated burning.

completeness on P mobility, three types of samples representing increasing degrees of combustion completeness produced from the same biomass were compared: (1) charcoal; (2) residues from simulated open burning (i.e. natural fire residue samples); and (3) ash (i.e. complete combustion product) (Fig. 5). The results showed that P becomes more mobile as burning completeness increases. For example, the fraction of Olsen-P increases from 10 to 70% for samples of spruce cone and from 10 to 40% for those of red oak wood at pH 8 (Fig. 5a). A similar trend was observed for pH 4.0 (Fig. 5b). We further correlated the Olsen-P with the C contents of a set of combustion samples (from simulated burning in the lab and industrial boilers that burn entirely woods), and the result showed that the Olsen-P decreases with increasing C content (Fig. 5c). The result clearly shows that P in charcoal is less soluble than P in ash, and

increasing combustion completeness may enhance P solubility and mobility.

Mechanisms of P transformation during burning and impacts on P mobility

Charcoal is the incomplete burning product of fires; it is a significant nutrient pool and different from the complete burning product, ash, in terms of chemical composition and property. This study advances the current understanding of P thermochemistry during charcoal formation and mechanisms of P mobilisation from charcoal, via thorough characterisation of P speciation and solution extractability across a wide range of charcoal types.

In terms of P speciation, our results show that although P is similarly mineralised among different samples during

charcoal formation, the resulting P speciation (i.e. molecular structure and complexation state) varies greatly among plant species and parts, which pinpoint the roles of starting P speciation and elemental stoichiometry. First, as shown in ³¹P NMR data, orthophosphate and pyrophosphate are the sole structures identified in the charcoal extracts, despite the diverse P structures (such as different organophosphates and polyphosphates) in the biomass feedstock (Fig. 1). The data first suggested that phosphate ester (O-R) and phosphoanhydride (P-O-P) bonds (existing in organophosphates and polyphosphates) are cleaved during pyrolysis, even at temperature as low as 300 °C. Varying abundances of pyrophosphate were identified (in spruce cone chars and white pine cone chars) and remained stable at the tested temperature range (300-600 °C). Pyrophosphate was also inconsistently detected in natural fire residues. For example, pyrophosphate accounts for about 0.2-2.8% of total extractable P in fire residues from a pine forest fire but is absent in the residue from a eucalypt forest fire (García-Oliva et al. 2018; Santín et al. 2018). Without information on the biomass composition and fire conditions, causes of this variation were unknown. Pyrophosphate could be potentially inherited from the starting biomass or formed from the polymerisation of phosphate molecules. Phytate is considered the precursor for pyrophosphate, as shown in studies on phytate-rich organic wastes such as manure and nut shell (Uchimiya et al. 2015). Our data suggested that phytate is not present in the starting biomass (Fig. 1a) and is unlikely to be the source of pyrophosphate in spruce cone charcoals. Instead, it is more likely to inherit from the biomass that contains pyrophosphate. Second, our result also suggests that the complexation state of P (complexation with metals such as Ca, Mg, K and Na, as well as mineralogy) is likely determined by both the starting P speciation and thermochemical reactions during biomass burning. Calcium and Mg phosphates were the main minerals identified by XANES, and their abundance increases with increasing metal to P molar ratios in the starting biomass (Fig. 2). With Ca and Mg being the most abundant metals in biomass, they are the most likely ones to form complex various P structures and remain unchanged during heating. However, cleavages of phosphate ester (O-R) and phosphoanhydride (P-O-P) bonds during heating induce changes to the complexation state, because the organic moieties and adjacent P will be replaced by a metal cation. The metal to replace organic moieties during organophosphate mineralisation may depend on its localised abundance and P-binding affinity. Therefore, variations in elemental stoichiometry and the abundance of organophosphates and condensed phosphates in biomass, as well as thermochemical reactions during heating, likely determine P speciation in charcoal.

Regarding P solubility, our results show that most P are likely entrapped physically in the C matrix, and the soluble P fraction is mostly inorganic phosphates that are mobilised through dissolution. Although P in charcoal exists mostly as

inorganic phosphates (as summarised above), only a small portion (less than 20% for most charcoals) was extractable by the sequential extraction solutions that include concentrated HCl. Charcoal is a carbonaceous porous material and a fraction of P is likely bound within the C matrix and not exposed to extraction solution, despite the soluble nature of the P species. The extractable P partitions are found mainly among H₂O, NaHCO₃ and HCl, along with the fast release kinetics of Olsen-P, suggesting that charcoal P is available mainly through solubilisation of inorganic phosphates on charcoal surface (Figs 3 and 4). However, the relative abundance of these P pools varies among charcoals, which is possibly controlled by their different P chemical forms and surface exposure. For example, spruce chars tend to have more soluble P than other chars formed at the same thermal condition, because of their low Ca/P ratios and potentially more soluble Mg and K phosphates. The matrix effect is reflected in varying P solubility among different T chars from the same biomass (Fig. 3). In general, charcoal becomes more aromatic and porous as heating temperature increases, whose effects on P solubility are counteractive. As a result of both chemical and physical factors, P solubility does not correlate simply to either surface P concentration or metal ratios (Fig. 4). The matrix effect is also manifested in enhanced P mobilisation as a result of complete burning, with more P being freed from the C matrix and its solubility depending primarily on the P chemical forms (Fig. 5).

Conclusion

This study advances our understanding of the chemistry and mobility of P in charcoal by characterising P chemical forms and solution extractability of charcoal from a wide range of plant species and compartments. The results demonstrate the great variations in P chemistry and solution extractability, as a result of highly variable P speciation and elemental stoichiometry in initial biomass, as well as the C matrix effect as a result of heating. The results also show enhanced P solubilisation with increasing combustion completeness, because ash P is free from physical constraints and more soluble than charcoal P. The results of this work have important implications with regard to evaluating the disturbance of fires to ecosystem P cycling, considering that vegetation fires occur in ecosystems with different vegetation composition and differ in severity.

Supplementary material

Supplementary material is available online.

References

Bayley SE, Schindler DW, Beaty KG, Parker BR, Stainton MP (1992) Effects of Multiple Fires on Nutrient Yields from Streams Draining

- Boreal Forest and Fen Watersheds: Nitrogen and Phosphorus. *Canadian Journal of Fisheries and Aquatic Sciences* **49**, 584–596. doi:10.1139/f92-068
- Bodí MB, Martin DA, Balfour VN, Santín C, Doerr SH, Pereira P, Cerdà A, Mataix-Solera J (2014) Wildland fire ash: Production, composition and eco-hydro-geomorphic effects. *Earth-Science Reviews* 130, 103–127. doi:10.1016/j.earscirev.2013.12.007
- Butler OM, Elser JJ, Lewis T, Mackey B, Chen CR (2018) The phosphorus-rich signature of fire in the soil-plant system: a global meta-analysis. *Ecology Letters* **21**, 335–344. doi:10.1111/ele.12896
- Cade-Menun BJ (2005) Characterizing phosphorus in environmental and agricultural samples by 31P nuclear magnetic resonance spectroscopy. *Talanta* 66, 359–371. doi:10.1016/j.talanta.2004.12.024
- Chien SH, Clayton WR (1980) Application of Elovich Equation to the Kinetics of Phosphate Release and Sorption in Soils. *Soil Science Society of America Journal* 44, 265–268. doi:10.2136/sssaj1980. 03615995004400020013x
- Doolette AL, Smernik RJ (2011) Soil Organic Phosphorus Speciation Using Spectroscopic Techniques. In 'Phosphorus in Action: Biological Processes in Soil Phosphorus Cycling'. (Eds E Bünemann, A Oberson, E Frossard) pp. 3–36. (Springer Berlin Heidelberg: Berlin, Heidelberg)
- Du E, Terrer C, Pellegrini AFA, Ahlström A, van Lissa CJ, Zhao X, Xia N, Wu X, Jackson RB (2020) Global patterns of terrestrial nitrogen and phosphorus limitation. *Nature Geoscience* **13**, 221–226. doi:10.1038/s41561-019-0530-4
- Galang MA, Markewitz D, Morris LA (2010) Soil phosphorus transformations under forest burning and laboratory heat treatments. *Geoderma* **155**, 401–408. doi:10.1016/j.geoderma.2009.12.026
- García-Oliva F, Merino A, Fonturbel MT, Omil B, Fernández C, Vega JA (2018) Severe wildfire hinders renewal of soil P pools by thermal mineralization of organic P in forest soil: Analysis by sequential extraction and 31P NMR spectroscopy. *Geoderma* **309**, 32–40. doi:10.1016/j.geoderma.2017.09.002
- Gray DM, Dighton J (2006) Mineralization of forest litter nutrients by heat and combustion. *Soil Biology and Biochemistry* **38**, 1469–1477. doi:10.1016/j.soilbio.2005.11.003
- Gu C, Dam T, Hart SC, Turner BL, Chadwick OA, Berhe AA, Hu Y, Zhu M (2020) Quantifying Uncertainties in Sequential Chemical Extraction of Soil Phosphorus Using XANES Spectroscopy. *Environmental Science & Technology* 54, 2257–2267. doi:10.1021/acs.est.9b05278
- Hart SC, DeLuca TH, Newman GS, MacKenzie MD, Boyle SI (2005) Postfire vegetative dynamics as drivers of microbial community structure and function in forest soils. *Forest Ecology and Management* **220**, 166–184. doi:10.1016/j.foreco.2005.08.012
- Hedley MJ, Stewart JWB, Chauhan BS (1982) Changes in Inorganic and Organic Soil Phosphorus Fractions Induced by Cultivation Practices and by Laboratory Incubations. *Soil Science Society of America Journal* 46, 970–976. doi:10.2136/sssaj1982.03615995004600050017x
- Hidaka A, Kitayama K (2011) Allocation of foliar phosphorus fractions and leaf traits of tropical tree species in response to decreased soil phosphorus availability on Mount Kinabalu, Borneo. *Journal of Ecology* **99**, 849–857. doi:10.1111/j.1365-2745.2011.01805.x
- Hou EQ, Luo YQ, Kuang YW, Chen CR, Lu XK, Jiang LF, Luo XZ, Wen DZ (2020) Global meta-analysis shows pervasive phosphorus limitation of aboveground plant production in natural terrestrial ecosystems. *Nature Communications* 11, 637. doi:10.1038/s41467-020-14492-w
- Huang R, Fang C, Lu X, Jiang R, Tang Y (2017) Transformation of Phosphorus during (Hydro)thermal Treatments of Solid Biowastes: Reaction Mechanisms and Implications for P Reclamation and Recycling. *Environmental Science & Technology* **51**, 10284–10298. doi:10.1021/acs.est.7b02011
- Marañón-Jiménez S, Castro J, Fernández-Ondoño E, Zamora R (2013) Charred wood remaining after a wildfire as a reservoir of macro- and micronutrients in a Mediterranean pine forest. *International Journal of Wildland Fire* **22**, 681–695. doi:10.1071/WF12030
- McEachern P, Prepas EE, Gibson JJ, Dinsmore WP (2000) Forest fire induced impacts on phosphorus, nitrogen, and chlorophyll a concentrations in boreal subarctic lakes of northern Alberta. *Canadian Journal of Fisheries and Aquatic Sciences* **57**, 73–81. doi:10.1139/f00-124
- Noack SR, McLaughlin MJ, Smernik RJ, McBeath TM, Armstrong RD (2014) Phosphorus speciation in mature wheat and canola plants as

- affected by phosphorus supply. *Plant and Soil* **378**, 125–137. doi:10.1007/s11104-013-2015-3
- Olsen SR (1954) 'Estimation of available phosphorus in soils by extraction with sodium bicarbonate.' (US Department of Agriculture)
- Pereira P, Úbeda X, Martin DA (2012) Fire severity effects on ash chemical composition and water-extractable elements. *Geoderma* **191**, 105–114. doi:10.1016/j.geoderma.2012.02.005
- Pistocchi C, Meszaros E, Tamburini F, Frossard E, Bunemann EK (2018) Biological processes dominate phosphorus dynamics under low phosphorus availability in organic horizons of temperate forest soils. *Soil Biology and Biochemistry* **126**, 64–75. doi:10.1016/j.soilbio.2018. 08.013
- Qian Y, Miao SL, Gu B, Li YC (2009) Effects of Burn Temperature on Ash Nutrient Forms and Availability from Cattail (Typha domingensis) and Sawgrass (Cladium jamaicense) in the Florida Everglades. *Journal of Environmental Quality* **38**, 451–464. doi:10.2134/jeq2008.0126
- Santin C, Otero XL, Doerr SH, Chafer CJ (2018) Impact of a moderate/high-severity prescribed eucalypt forest fire on soil phosphorous stocks and partitioning. *Science of the Total Environment* **621**, 1103–1114. doi:10.1016/j.scitotenv.2017.10.116
- Schaller J, Tischer A, Struyf E, Bremer M, Belmonte DU, Potthast K (2015) Fire enhances phosphorus availability in topsoils depending on binding properties. *Ecology* **96**, 1598–1606. doi:10.1890/14-1311.1
- Smith AP, Fontenot EB, Zahraeifard S, DiTusa SF (2015) Molecular Components That Drive Phosphorus-Remobilisation during Leaf Senescence. In 'Phosphorus Metabolism in Plants. Vol. 48'. (Eds WC Plaxton, H Lambers) pp. 160–186. (John Wiley & Sons, Ltd)
- Sohrt J, Lang F, Weiler M (2017) Quantifying components of the phosphorus cycle in temperate forests. *WIREs Water* 4, e1243. doi:10.1002/wat2.1243
- Sun K, Qiu MY, Han LF, Jin J, Wang ZY, Pan ZZ, Xing BS (2018) Speciation of phosphorus in plant- and manure-derived biochars and its dissolution under various aqueous conditions. *Science of The Total Environment* **634**, 1300–1307. doi:10.1016/j.scitotenv.2018. 04.099
- Turner BL, Mahieu N, Condron LM (2003) Phosphorus-31 nuclear magnetic resonance spectral assignments of phosphorus compounds in soil NaOH-EDTA extracts. *Soil Science Society of America Journal* **67**, 497–510. doi:10.2136/sssaj2003.4970
- Turner BL, Condron LM, Richardson SJ, Peltzer DA, Allison VJ (2007) Soil organic phosphorus transformations during pedogenesis. *Ecosystems* **10**, 1166–1181. doi:10.1007/s10021-007-9086-z
- Úbeda X, Pereira P, Outeiro L, Martin DA (2009) Effects of fire temperature on the physical and chemical characteristics of the ash from two plots of cork oak (Quercus suber). *Land Degradation & Development* **20**, 589–608. doi:10.1002/ldr.930
- Uchimiya M, Hiradate S (2014) Pyrolysis Temperature-Dependent Changes in Dissolved Phosphorus Speciation of Plant and Manure Biochars. *Journal of Agricultural and Food Chemistry* **62**, 1802–1809. doi:10.1021/jf4053385
- Uchimiya M, Hiradate S, Antal MJ (2015) Dissolved Phosphorus Speciation of Flash Carbonization, Slow Pyrolysis, and Fast Pyrolysis Biochars. *ACS Sustainable Chemistry & Engineering* **3**, 1642–1649. doi:10.1021/acssuschemeng.5b00336
- Werner F, Prietzel J (2015) Standard Protocol and Quality Assessment of Soil Phosphorus Speciation by P K-Edge XANES Spectroscopy. *Environmental Science & Technology* **49**, 10521–10528. doi:10.1021/acs.est.5b03096
- Wu Y, Pae LM, Gu C, Huang R (2023) Phosphorus Chemistry in Plant Ash: Examining the Variation across Plant Species and Compartments. *ACS Earth and Space Chemistry* **7**, 2205–2213. doi:10.1021/acsearthspacechem.3c00145
- Xu G, Zhang Y, Shao H, Sun J (2016) Pyrolysis temperature affects phosphorus transformation in biochar: Chemical fractionation and 31P NMR analysis. *Science of The Total Environment* **569-570**, 65–72. doi:10.1016/j.scitotenv.2016.06.081
- Yu L, Zanchi G, Akselsson C, Wallander H, Belyazid S (2018) Modeling the forest phosphorus nutrition in a southwestern Swedish forest site. *Ecological Modelling* **369**, 88–100. doi:10.1016/j.ecolmodel.2017. 12.018

Data availability. All data will be made available upon request to the authors.

Conflicts of interest. The authors declare no conflicts of interest.

Declaration of funding. This work was supported by the National Science Foundation (#2120547) and Startup funds from University at Albany.

Acknowledgements. The authors thank beamline scientists at Brookhaven National Laboratory, Dr. Yonghua Du and Dr. Seongmin Bak for helping with experimental setup and XANES data collection. This research used 8-BM of the National Synchrotron Light Source II, a US Department of Energy (DOE) Office of Science User Facility operated for the DOE Office of Science by Brookhaven National Laboratory under Contract No. DE-SC0012704. We also thank Dr. Jeremy I. Feldblyum and his group in the department of chemistry at University at Albany for measuring specific surface area of the charcoal samples.

Author affiliation

^ADepartment of Environmental and Sustainable Engineering, University at Albany, 1400 Washington Avenue, Albany, NY 12222, USA.